Earth Syst. Dynam. Discuss., doi:10.5194/esd-2016-4, 2016
Manuscript under review for journal Earth Syst. Dynam.
Published: 22 February 2016

Earth System Dynamics
Discussions
Open Access
EGU

Spatial and temporal variations in plant Water Use Efficiency inferred from tree-ring, eddy covariance and atmospheric observations

Margriet Groenendijk[1], Peter M. Cox[1], Ben B. B. Booth[2], Stefan C. Dekker[3] and Chris Huntingford[4]

[1] *College of Engineering, Mathematics and Physical Sciences, University of Exeter, North Park Road, Exeter, EX4 4QF, UK*

[2] *Met Office Hadley Centre, FitzRoy Road, Exeter, EX1 3PB, UK*

[3] *Copernicus Institute of Sustainable Development, Faculty of Geosciences, Utrecht University, Heidelberglaan 2, 3584 CS Utrecht, the Netherlands*

[4] *Centre for Ecology and Hydrology, Benson Lane, Wallingford, OXON, OX10 8BB, UK*

Author contributions: M.G. and P.M.C. designed the study; M.G. compiled the datasets and performed the analysis; M.G. and P.M.C. drafted the manuscript; M.G. P.M.C., S.C.D., B.B.B. and C.H. have had many discussions that shaped the research. All authors commented on and provided edits to the manuscript.

Earth Syst. Dynam. Discuss., doi:10.5194/esd-2016-4, 2016
Manuscript under review for journal Earth Syst. Dynam.
Published: 22 February 2016

Earth System Dynamics Discussions
Open Access
EGU

Abstract

Plant Water Use Efficiency (*WUE*), which is the ratio of the uptake of carbon dioxide through photosynthesis to the loss of water through transpiration, is a very useful metric of the functioning of the land biosphere. *WUE* is expected to increase with atmospheric CO_2, but to decline with increasing atmospheric evaporative demand – which can arise from increases in near-surface temperature or decreases in relative humidity. We have used $\Delta^{13}C$ measurements from tree-rings, along with eddy-covariance measurements from Fluxnet sites, to estimate the sensitivities of WUE to changes in CO_2 and atmospheric humidity deficit. This enables us to reconstruct fractional changes in *WUE*, based on changes in atmospheric climate and CO_2, for the entire period of the instrumental global climate record. We estimate that overall *WUE* increased from 1900 to 2010 by 48±22%, which is more than double that simulated by the latest Earth System Models. This long-term trend is largely driven by increases in CO_2, but significant inter-annual variability and regional differences are evident due to variations in temperature and relative humidity. There are several highly populated regions, such as Western Europe and East Asia, where the rate of increase of *WUE* has declined sharply in the last two decades.

Earth Syst. Dynam. Discuss., doi:10.5194/esd-2016-4, 2016
Manuscript under review for journal Earth Syst. Dynam.
Published: 22 February 2016

Earth System Dynamics Discussions
Open Access
EGU

1. Introduction

Plant Water Use Efficiency (*WUE*) is the ratio of the CO_2 assimilated through photosynthesis (Gross Primary Productivity, *GPP*), to the water used by plants as the flux of Transpiration (E_T):

$$WUE = \frac{GPP}{E_T} \quad (1)$$

Carbon dioxide may affect plants through increases in photosynthesis (Ainsworth and Rogers 2007; Franks et al. 2013) and possible reductions in transpiration associated with the partial closure of leaf stomatal pores under elevated CO_2 (Field et al. 1995; Gedney et al. 2006; Betts et al. 2007). Both of these effects are uncertain though. CO_2-fertilization of photosynthesis is often found to be limited by nutrient availability (Norby et al. 2010), and large-scale transpiration may not reduce even with CO_2-induced stomatal closure, if plant leaf area index increases enough to counteract reduced transpiration from each leaf (Piao et al. 2007). *WUE* does however appear to be increasing more robustly with CO_2, according to both tree-ring (Franks et al. 2013) and eddy-covariance flux measurements (Keenan et al. 2013).

Plant photosynthesis and transpiration are coupled through the behaviour of leaf stomatal pores, through which CO_2 must diffuse to be fixed during photosynthesis, and through which the transpiration flux escapes to the atmosphere. The combined behaviour of the leaf stomata leads to an environmentally dependent "canopy conductance" that controls both the water and carbon fluxes. As a consequence, both *GPP* and E_T can be written as the product of a canopy conductance

Earth Syst. Dynam. Discuss., doi:10.5194/esd-2016-4, 2016
Manuscript under review for journal Earth Syst. Dynam.
Published: 22 February 2016

Earth System Dynamics Discussions
Open Access
EGU

and a concentration gradient, which is sometimes described as an electrical analogue (Cowan 1972). For *GPP*, the concentration gradient is the difference between the atmospheric CO_2 concentration at the leaf surface (C_a) and the internal CO_2 concentration within plant leaves (C_i):

$$GPP = g_c(C_a - C_i) \quad (2)$$

where g_c is the canopy conductance for CO_2.

For E_T, the concentration gradient is the difference between the specific humidity of the atmosphere at the leaf surface (q_a) and the specific humidity inside the plant leaves, which is saturated at the surface temperature (q_{sat}). The canopy conductances for *GPP* and E_T both arise from diffusion through leaf stomatal pores, and therefore only differ by a constant factor of 1.6 (the square root of the ratio of the molecular masses of CO_2 and H_2O).

$$E_T = 1.6 g_c(q_{sat} - q_a) \quad (3)$$

Changes in stomatal opening in response to changes in sunlight, atmospheric temperature and humidity, soil moisture, and CO_2, are complex and uncertain (Berry et al. 2010), as are the scaling of these leaf-level responses up to the canopy and beyond (Piao et al. 2007; Jarvis and McNaughton 1986; Jarvis 1995). However, since stomatal behaviour affects transpiration and photosynthesis similarly, *WUE* is relatively insensitive to these uncertainties:

$$WUE = \frac{(C_a - C_i)}{1.6(q_{sat} - q_a)} = \frac{(C_a - C_i)}{1.6D} = \frac{C_a(1-f)}{1.6D} \quad (4)$$

Earth Syst. Dynam. Discuss., doi:10.5194/esd-2016-4, 2016
Manuscript under review for journal Earth Syst. Dynam.
Published: 22 February 2016

Earth System Dynamics Discussions
Open Access
EGU

where D is the atmospheric humidity deficit (q_{sat}-q_a) and f is the ratio of the internal to the external CO_2 concentration (C_i/C_a). This equation therefore expresses WUE in terms of atmospheric variables, C_a and D (which itself depends on relative humidity and temperature), along with the factor f. The remaining uncertainty associated with plant physiology is therefore contained in f.

In the absence of water limitations, there is good evidence that f is approximately independent of C_a, so that C_i remains proportional to C_a, unless D changes (Jacobs 1994; Katul et al. 2010; Leuning 1995; Morison et al. 1983). Even during drought, f will vary with D, due in part to correlations between D and soil moisture (Brodribb 1996).

Stomatal optimisation theories, which assume that stomata act so as to maximise photosynthesis for a given amount of available water (Cowan and Farquhar 1977), also suggest that f should depend predominantly on C_a and D (Katul et al. 2010; Medlyn et al. 2011). Absolute values of WUE will depend on the nature of the vegetation and soil, such as the plant and soil hydraulics, but these optimisation theories imply that there will be a near universal sensitivity of fractional changes in WUE to fractional changes in C_a and D (see SI Appendix):

$$\frac{WUE}{WUE(0)} = \left(\frac{C_a}{C_a(0)}\right)^a \left(\frac{D}{D(0)}\right)^b \quad (5)$$

where the subscript (0) denotes the initial state of each variable, and a and b are dimensionless coefficients. For given a and b values this equation describes how the fractional change in WUE at each location varies with fractional changes in C_a and D. Although they differ in their underlying

Earth Syst. Dynam. Discuss., doi:10.5194/esd-2016-4, 2016
Manuscript under review for journal Earth Syst. Dynam.
Published: 22 February 2016

assumptions and detailed conclusions, it is interesting to note that the latest stomatal optimization theories (Katul et al. 2010; Medlyn et al. 2011) both imply $a=1$ and $b=-0.5$ (see SI Appendix).

We focus in this study on fractional changes in *WUE*, which are more likely to be independent of these complex factors. We do not assume the applicability of stomatal optimization theories, but instead adopt equation 5 as a parsimonious empirical model for the fractional changes in *WUE* observed at each measurement site, given suitable fitting parameters a and b. Tests using more elaborate statistical models, with additional environmental variables or vegetation-specific parameters, were not found to produce significant improvements in the fit to the observed changes in WUE despite the introduction of extra fitting parameters.

Earth Syst. Dynam. Discuss., doi:10.5194/esd-2016-4, 2016
Manuscript under review for journal Earth Syst. Dynam.
Published: 22 February 2016

2. Materials and Methods

We estimate the sensitivity of *WUE* to C_a and D by fitting to *WUE* changes inferred from both eddy-covariance fluxes (relatively short records with high-temporal resolution) and carbon isotope records from tree-rings (longer-term records with annual resolution). We use observations from 28 eddy-covariance and 31 tree-ring sites (see SI Appendix, Fig. S1 and Tables S1 and S2).

2.1 Eddy-covariance observations.

The carbon and water flux observations were taken from the *Free Fair-use* Fluxnet database (www.fluxdata.org) (Baldocchi 2008; Papale et al. 2006; Reichstein et al. 2005). We selected a total of 28 sites based on data availability (see SI Appendix, Fig. S1 and Table S1). Monthly *WUE* was estimated from Equation 1 with *GPP* used directly from the database (Reichstein et al. 2005). In general the total latent heat flux (*LE*) has contributions from interception loss, soil evaporation and transpiration. We follow previous studies (Groenendijk et al. 2011; Keenan et al. 2013; Law et al. 2002) in assuming that the latent heat flux is dominated by transpiration during periods with no rain in the preceding two days, when the interception loss and soil evaporation are assumed small. Monthly average values of *GPP*, E_T, C_a, D and T were calculated from half-hourly observations (not gap-filled) during dry periods (*i.e.* no rain in the preceding two days) when *GPP* was larger than zero. To exclude periods with unrealistic *WUE* values due to the division by very small E_T values, we used only months during the growing season. Annual average growing season values were calculated from the months with an average temperature above 10^{o}C. Only sites with at least 6 annual values were used, resulting in a dataset of 222 annual growing season values of *WUE*, C_a and D. Fractional changes were calculated relative to the mean over the observational period for each of the sites, to enable comparison between sites.

Earth Syst. Dynam. Discuss., doi:10.5194/esd-2016-4, 2016
Manuscript under review for journal Earth Syst. Dynam.
Published: 22 February 2016

Earth System Dynamics
Discussions
Open Access
EGU

138 **2.2. Tree-ring observations**.

139 To derive a longer-term relationship between the fractional change in *WUE* and variations in C_a and
140 D, we used $\Delta^{13}C$ tree-ring observations from 31 locations as described in two previous studies
141 (Franks et al. 2013, Hemming et al. 1998) (see SI Appendix, Table S2). The discrimination of ^{12}C
142 against ^{13}C ($\Delta^{13}C$) is estimated from the tree-ring samples (Hemming et al. 1998; van der Sleen et
143 al. 2015). The $\Delta^{13}C$ measurements can be used to estimate the ratio of the internal to the external
144 CO_2 concentration ($f=C_i/C_a$) using the relationship: $f = (\Delta^{13}C - 4.4)/ (27-4.4)$, where $\Delta^{13}C$ is in parts
145 per thousand (‰), and C_a is taken from the Mauna Loa atmospheric CO_2 record (Farquhar et al.
146 1989; Franks et al. 2013; Keeling et al. 1976). *WUE* is estimated with Equation 2 using annual
147 average growing season values of D from the CRU dataset, taking the nearest pixel to each site
148 (Harris et al. 2013). This large-scale dataset for D ensures consistency among the sites, but may
149 underestimate the finer spatial variation in D. As for the eddy-covariance sites, we estimated the
150 fractional changes relative to the mean over the observational period at each of the sites. For this
151 analysis we have 1007 observations of *WUE* derived from tree-ring observations of $\Delta^{13}C$.
152
153

Earth Syst. Dynam. Discuss., doi:10.5194/esd-2016-4, 2016
Manuscript under review for journal Earth Syst. Dynam.
Published: 22 February 2016

Earth System Dynamics Discussions Open Access EGU

3 Results and Discussion

Figure 1 summarises the derivation of the a and b parameters, which are the sensitivity of WUE to C_a and D, for the tree-ring and eddy-covariance observations. To estimate a and b with a linear regression model we rewrite Equation 3 in a logarithmic form:

$$\ln\left\{1+\frac{\Delta WUE}{WUE(0)}\right\} = a\ln\left\{1+\frac{\Delta C_a}{C_a(0)}\right\} + b\ln\left\{1+\frac{\Delta D}{D(0)}\right\} \quad (6)$$

Here the second-term in each bracket represents the fractional change in WUE, C_a and D, respectively. These fractional change variables are used in all our subsequent statistical analyses and modelling. We set out to fit the fractional change in WUE at each observation site from the fractional change in C_a and the fractional change in D. For comparison and fitting we therefore need to calculate $WUE(0)$, $C_a(0)$ and $D(0)$ for the observational data, which we take as the mean over the entire observational record available at each site.

In general, eddy-covariance data alone is unable to fully constrain the CO_2 sensitivity of the WUE (Keenan et al. 2013), because the data records are too short to sample significant changes in CO_2, resulting in a value of a of 0.79±0.79 for all eddy-covariance site (SI Appendix, Fig. S2 and Table S3). However, the longer tree-ring records overall yield a good constraint on a of 1.61±0.54. The annual data-points for the two datasets can be combined into a single dataset. Fitting against this more complete dataset gives generic sensitivity coefficients of a=1.51±0.57 and b=-0.72±0.16. These values are mainly constrained by the tree-ring observations for which the fits to equation 6 are more tightly defined (SI Appendix, Fig S2a). This value of a suggests that WUE has been increasing even faster than the atmospheric CO_2 concentration (Fig. 1a). This is qualitatively

Earth Syst. Dynam. Discuss., doi:10.5194/esd-2016-4, 2016
Manuscript under review for journal Earth Syst. Dynam.
Published: 22 February 2016

consistent with conclusions from a previous study, which was based purely on eddy covariance data (Keenan et al. 2013), but is more robustly demonstrated here due to the much longer tree-ring records.

It is interesting to note that our overall values of a=1.51±0.57 and b=-0.72±0.16 are larger by about 50% than the values derived from stomatal optimization theories: a=1.0, b=-0.5 (Cowan and Farquhar 1977; Katul et al. 2010; Palmroth et al. 2013, 16, 19, 30), indicating a stronger response to changes in both CO_2 and climate. Such theoretical sensitivities are common to variants of stomatal optimization theory, including those that assume either electron transport-limited or Rubisco-limited photosynthesis, and even when additional nitrogen limitations are accounted for (Prentice et al. 2013). The differences between the optimization theory and our empirically derived *WUE* sensitivities may arise from differences between leaf-surface and atmospheric values of CO_2 and humidity, but they may also be indicative of missing constraints in the optimization theories (Lin et al. 2015; Prentice et al. 2014).

Testing more elaborate statistical models.

Equation 6 is motivated by empirical evidence and theory suggesting that *WUE* should vary predominantly with C_a and D. However, it is conceivable that the fractional change in *WUE* could also depend on other environmental conditions or the detailed vegetation type. In order to test for this, we carried out two additional sets of fits against the observational data. In the first test we extended our statistical model (equation 6) to include other environmental variables that had been measured at the *Fluxnet* sites, most notably solar radiation, air temperature, and soil water content. Including these additional predictor variables does not significantly improve the fit to the observed

Earth Syst. Dynam. Discuss., doi:10.5194/esd-2016-4, 2016
Manuscript under review for journal Earth Syst. Dynam.
Published: 22 February 2016

changes in *WUE* (as measured by r^2), and typically results in less robust predictions (as measured by the adjusted r^2), because of the introduction of extra fitting parameters (SI Appendix, Table S4). In the second test, we carried out separate statistical fits for each of the sites listed in the *Fluxnet* dataset. Clustering of these values by vegetation type would indicate that *a* and *b* parameters are dependent on vegetation type, but we find no evidence of such clustering (SI Appendix, Fig. S7).

Comparison to independent *WUE* estimates.

Our best-fit generic *a* and *b* parameters are able to reasonably reproduce the fractional changes in *WUE* due to fractional changes in both C_a and *D* across the 59 tree-ring and eddy-covariance sites (SI Appendix, Fig. S3). However, it is important to evaluate the estimated response of *WUE* to C_a and *D* against independent data. We compared the change in *WUE* estimated with the best-fit parameters to observations at three tropical tree-ring sites from a recent study (van der Sleen et al. 2015). At these sites a range of species of both trees and under-storey were sampled. Our estimate for these three locations passes close to the mean of the observed *WUE* fractional changes (Fig. 2a-c). In addition we compared our estimated change in *WUE* to changes derived from a remote sensing (RS) product of *GPP* and E_T (Jung et al. 2011). This dataset covers the period 1982-2006; we use the period 1986-1990 as a reference period for both our estimate and the fractional change in *WUE* from the RS product. Because the RS data does not include a response to changes in C_a, we estimated a fractional change in *WUE* with and without this response (Fig. 2d-f) for three regions, which show distinct changes in *WUE*: Western North America, Western Europe and East Asia. The RS fluxes show little inter-annual variability, and much less variability than we estimate. For the three regions in Fig. 2d-f our estimates with and without CO_2 effects sit on either side of the RS estimates. In other regions (see SI Appendix, Fig. S4) our estimates excluding CO_2 effects are

Earth Syst. Dynam. Discuss., doi:10.5194/esd-2016-4, 2016
Manuscript under review for journal Earth Syst. Dynam.
Published: 22 February 2016

Earth System Dynamics Discussions
Open Access
EGU

223 similar to the RS estimates, whilst the inclusion of CO_2 effects leads to significant increases in
224 WUE (SI Appendix, Fig. S5) that appear to be inconsistent with the RS estimates (which do not
225 account for CO_2 changes), but are more consistent with the tree-ring (Franks et al. 2013) and eddy-
226 covariance data (Keenan et al. 2013).
227
228 **Global fractional change of *WUE***.
229 The dependence of fractional changes in *WUE* on C_a and *D* allows us to use these relationships to
230 estimate changes in *WUE* at large scales using global climate data. The fractional change in *D* can
231 be further partitioned into a change in temperature (*T*) and relative humidity (*RH*), which makes it
232 possible to separate the effect of changes in these variables on *WUE* (see SI Appendix). To do this,
233 we used the CRU climate dataset (Harris et al. 2013) at a $0.5^o \times 0.5^o$ latitude/longitude grid and the
234 annual CO_2 concentration at Mauna-Loa (Keeling et al. 1976) to derive the global and local
235 variation in *WUE*. We only used months during the growing season when photosynthesis occurs,
236 assumed to be above a monthly average temperature threshold of 10^oC as for the eddy-covariance
237 sites. For the period 1900-1930 the average temperature was calculated for each month from which
238 a spatial mask was generated (SI Appendix, Fig. S6). This mask was then used to calculate annual
239 time-evolving values of *WUE* from the growing season values of temperature and humidity for each
240 year between 1901 and 2010.
241
242 Globally, we estimate that *WUE* has increased by 48±22% since 1900 (Fig. 3a), with the CO_2
243 increase contributing +47±21% and relative humidity contributing +3.6±1.3%, counteracted by a
244 much smaller reduction in *WUE* due to warming of -2.3±0.8%. Uncertainties in global *WUE*

Earth Syst. Dynam. Discuss., doi:10.5194/esd-2016-4, 2016
Manuscript under review for journal Earth Syst. Dynam.
Published: 22 February 2016

changes were derived from the range of the parameters *a* and *b* within 5% of the RMSE of our best fit (Fig. 1c).

Comparison to simulations with complex Earth System Models (ESMs).

Most of the latest ESMs calculate changes in both GPP and transpiration. This allows a comparable change in *WUE* to be calculated for 28 CMIP5 models (Taylor et al. 2012) based-on their historical simulations. The CMIP5 models simulate an increase in *WUE* of between 2% and 28% to 2005, with an ensemble mean of 14% (SI Appendix, Table S5). For comparison, our overall fit against the tree-ring and eddy-covariance data indicates an approximately 40% increase in *WUE* over the same period. Figure 4 compares the annual time-series of the fractional changes in *WUE* from the CMIP5 models (black line and green uncertainty plumes), our statistical fit (orange lines), and the mean changes observed for the tree-ring (black marks and grey uncertainty bars) and eddy-covariance sites (dark blue marks and light blue uncertainty bars). This comparison suggests that the latest ESMs significantly underestimate the historical increase in *WUE*.

Regional changes in *WUE*.

Our global average change in *WUE* hides substantial regional differences (Fig. 3b). This is a result of the spatially and temporally varying impact of climate change on *WUE* (Fig. 5a and animation in the Supporting Information), driven by the heterogeneity of the warming (Fig. 5b) and the large variation in changes in near-surface *RH* (Fig. 5c). In many regions the overall impact is a significant increase in *WUE*, such as Western North America (Fig. 5d). However, the recent rate of increase has declined substantially in several heavily populated regions. For example, *WUE* shows a slower increase in Western Europe since the 1980s, as a result of increases in *T*, which has counteracted the

Earth Syst. Dynam. Discuss., doi:10.5194/esd-2016-4, 2016
Manuscript under review for journal Earth Syst. Dynam.
Published: 22 February 2016

268 *WUE* increase due to increasing CO_2 (Fig. 5e). This is also observed in *WUE* trends derived from
269 isotopic tree-ring observations in Spain (Linares et al. 2012). Our analysis indicates that East Asia
270 has suffered an even more significant suppressions of *WUE* since about 1990, due predominantly to
271 reductions in *RH* (Wang et al. 2012) (Fig. 5f). This pattern of changing *RH* is comparable with the
272 trends in precipitation and drought since 1950 (Dai 2011).
273
274

Earth Syst. Dynam. Discuss., doi:10.5194/esd-2016-4, 2016
Manuscript under review for journal Earth Syst. Dynam.
Published: 22 February 2016

4. Conclusions

This study shows that fractional changes in plant *WUE*, at large-scales and over the period of the climatological record, can be inferred from atmospheric data alone. By combining two very different datasets of WUE derived from tree-ring $\Delta^{13}C$ measurements and eddy-covariance fluxes we have derived a consistent response of the fractional change in *WUE* to the fractional changes in C_a and D. This generic response can be used to estimate the global WUE changes. Our analysis shows that global *WUE* increased by approximately a half over the 20th century predominantly due to rising CO_2, which is significantly more than is simulated by the latest Earth System Models. However, this increase in *WUE* has been modulated downwards in recent decades by the impact of climate change. This is especially true for the highly populated regions of Western Europe and East Asia, where reductions in atmospheric relative humidity and increases in temperature have acted to offset increases in *WUE* due to increasing CO_2. We conclude that the effects of increasing CO_2 on plant *WUE* are significantly underestimated in the latest climate projections.

ACKNOWLEDGEMENTS

The contributions of M.G. and C.H were funded by the UK Natural Environment Research Council (NERC) HYDRA project. We thank Margaret Barbour for providing us tree-ring data compiled from many different sources. This work used eddy-covariance data acquired by the FLUXNET community and in particular by the following networks: AmeriFlux (U.S. Department of Energy, Biological and Environmental Research, Terrestrial Carbon Program (DE-FG02-04ER63917 and DE-FG02-04ER63911)), AfriFlux, AsiaFlux, CarboAfrica, CarboEuropeIP, CarboItaly,

Earth Syst. Dynam. Discuss., doi:10.5194/esd-2016-4, 2016
Manuscript under review for journal Earth Syst. Dynam.
Published: 22 February 2016

299 CarboMont, ChinaFlux, Fluxnet-Canada (supported by CFCAS, NSERC, BIOCAP, Environment
300 Canada, and NRCan), GreenGrass, KoFlux, LBA, NECC, OzFlux, TCOS-Siberia, USCCC. We
301 acknowledge the financial support to the eddy covariance data harmonization provided by
302 CarboEuropeIP, FAO-GTOS-TCO, iLEAPS, Max Planck Institute for Biogeochemistry, National
303 Science Foundation, University of Tuscia, Université Laval and Environment Canada and US
304 Department of Energy and the database development and technical support from Berkeley Water
305 Center, Lawrence Berkeley National Laboratory, Microsoft Research eScience, Oak Ridge National
306 Laboratory, University of California - Berkeley, University of Virginia.
307

Earth Syst. Dynam. Discuss., doi:10.5194/esd-2016-4, 2016
Manuscript under review for journal Earth Syst. Dynam.
Published: 22 February 2016

308

309 **References**

310

311

312 Ainsworth EA, Rogers A (2007) The response of photosynthesis and stomatal conductance to rising
313 [CO2]: mechanisms and environmental interactions. Plant Cell Environ 30:258–270.
314 Baldocchi DD (2008) Breathing of the terrestrial biosphere: lessons learned from a global network
315 of carbon dioxide flux measurement systems. Aust J Bot 56:1–26.
316 Berry J, Beerling DJ, Franks PJ (2010) Stomata: key players in the earth system, past and present.
317 Curr Opin Plant Biol 13:233–240.
318 Betts RA et al. (2007) Projected increase in continental runoff due to plant responses to increasing
319 carbon dioxide. Nature 448:1037–U5.
320 Brodribb T (1996) Dynamics of changing intercellular CO2 concentration (ci) during drought and
321 determination of minimum functional ci. Plant Physiol 111:179–185.
322 Cowan I, Farquhar G (1977) Stomatal function in relation to leaf metabolism and environment. Soc
323 Exp Biol Symp 31:471–505.
324 Cowan IR (1972) An electrical analogue of evaporation from, and flow of water in plants. Planta
325 106:221–226.
326 Dai A (2011) Drought under global warming: a review. Wires Clim Change 2:45–65.
327 Farquhar G, Ehleringer JR, Hubick KT (1989) Carbon isotope discrimination and photosynthesis.
328 Annu Rev Plant Physiol Plant Mol Biol 40:503–537.
329 Field CB, Jackson RB, Mooney H (1995) Stomatal responses to increased CO2: implications from
330 the plant to the global-scale. Plant Cell Environ 18:1214–1225.

Earth Syst. Dynam. Discuss., doi:10.5194/esd-2016-4, 2016
Manuscript under review for journal Earth Syst. Dynam.
Published: 22 February 2016

331 Franks PJ et al. (2013) Sensitivity of plants to changing atmospheric CO2 concentration: from the
332 geological past to the next century. New Phytol 197:1077–1094.
333 Gedney N et al. (2006) Detection of a direct carbon dioxide effect in continental river runoff
334 records. Nature 439:835–838.
335 Groenendijk M et al. (2011) Seasonal variation of photosynthetic model parameters and leaf area
336 index from global Fluxnet eddy covariance data. J Geophys Res 116.
337 Harris I, Jones PD, Osborn TJ, Lister DH (2013) Updated high-resolution grids of monthly climatic
338 observations-the CRU TS3.10 Dataset. Int J Climatol.
339 Hemming DI, Switsur VR, Waterhouse JS, Heaton THE, Carter AHC (1998) Climate variation and
340 the stable carbon isotope composition of tree ring cellulose: an intercomparison of Quercus
341 robur , Fagus sylvatica and Pinus silvestris. Tellus B 50.
342 Jacobs CMJ (1994) Direct impact of atmospheric CO2 enrichment on regional transpiration.
343 Dissertation (Wageningen).
344 Jarvis PG (1995) Scaling processes and problems. Plant Cell Environ 18:1079–1089.
345 Jarvis PG, McNaughton KG (1986) Stomatal control of transpiration - Scaling up from leaf to
346 region. Adv Ecol Res 15:1–49.
347 Jung M et al. (2011) Global patterns of land-atmosphere fluxes of carbon dioxide, latent heat, and
348 sensible heat derived from eddy covariance, satellite, and meteorological observations. J
349 Geophys Res 116.
350 Katul G, Manzoni S, Palmroth S, Oren R (2010) A stomatal optimization theory to describe the
351 effects of atmospheric CO2 on leaf photosynthesis and transpiration. Annals of Botany 105:431–
352 442.

Earth Syst. Dynam. Discuss., doi:10.5194/esd-2016-4, 2016
Manuscript under review for journal Earth Syst. Dynam.
Published: 22 February 2016

353 Keeling CD et al. (1976) Atmospheric carbon dioxide variations at Mauna Loa Observatory,
354 Hawaii. Tellus 28:538–551.
355 Keenan TF et al. (2013) Increase in forest water-use efficiency as atmospheric carbon dioxide
356 concentrations rise. Nature 499:324–327.
357 Law BE et al. (2002) Environmental controls over carbon dioxide and water vapor exchange of
358 terrestrial vegetation. Agric For Meteorol 113:97–120.
359 Leuning R (1995) A critical appraisal of a combined stomatal-photosynthesis model for C3 plants.
360 Plant Cell Environ 18:339–355.
361 Lin Y-S et al. (2015) Optimal stomatal behaviour around the world. Nature Climate change.
362 Linares JC, Camarero JJ (2012) From pattern to process: linking intrinsic water-use efficiency to
363 drought-induced forest decline. Global Change Biol 18:1000–1015.
364 Medlyn BE et al. (2011) Reconciling the optimal and empirical approaches to modelling stomatal
365 conductance. Global Change Biol 17:2134–2144.
366 Morison JIL, Gifford RM (1983) Stomatal sensitivity to carbon dioxide and humidity. Plant Physiol
367 71:789–796.
368 Norby RJ, Warren JM, Iversen CM, Medlyn BE, McMurtrie RE (2010) CO2 enhancement of forest
369 productivity constrained by limited nitrogen availability. P Natl Acad Sci Usa 107:19368–19373.
370 Palmroth S et al. (2013) On the complementary relationship between marginal nitrogen and water-
371 use efficiencies among Pinus taeda leaves grown under ambient and CO2-enriched
372 environments. Annals of Botany 111:467–477.
373 Papale D et al. (2006) Towards a standardized processing of Net Ecosystem Exchange measured
374 with eddy covariance technique: algorithms and uncertainty estimation. Biogeosciences 3:571–
375 583.

Earth Syst. Dynam. Discuss., doi:10.5194/esd-2016-4, 2016
Manuscript under review for journal Earth Syst. Dynam.
Published: 22 February 2016

376 Piao SL et al. (2007) Changes in climate and land use have a larger direct impact than rising CO2
377 on global river runoff trends. P Natl Acad Sci Usa 104:15242–15247.
378 Prentice IC, Dong N, Gleason SM, Maire V, Wright IJ (2014) Balancing the costs of carbon gain
379 and water transport: testing a new theoretical framework for plant functional ecology. Ecol
380 Letters 17:82–91.
381 Reichstein M et al. (2005) On the separation of net ecosystem exchange into assimilation and
382 ecosystem respiration: review and improved algorithm. Global Change Biol 11:1424–1439.
383 Taylor KE, Stouffer RJ, Meehl G (2012) An Overview of CMIP5 and the Experiment Design, Bull.
384 Am. Meteorol. Soc., 93, 485–498, doi:10.1175/BAMS-D-11-00094.1.
385 van der Sleen P et al. (2015) No growth stimulation of tropical trees by 150 years of CO2
386 fertilization but water-use efficiency increased. Nature Geoscience 8:24–28.
387 Wang K, Dickinson RE, Liang S (2012) Global atmospheric evaporative demand over land from
388 1973 to 2008. J Climate 25:8353–8361.
389
390

Earth Syst. Dynam. Discuss., doi:10.5194/esd-2016-4, 2016
Manuscript under review for journal Earth Syst. Dynam.
Published: 22 February 2016

Earth System Dynamics
Discussions
Open Access
EGU

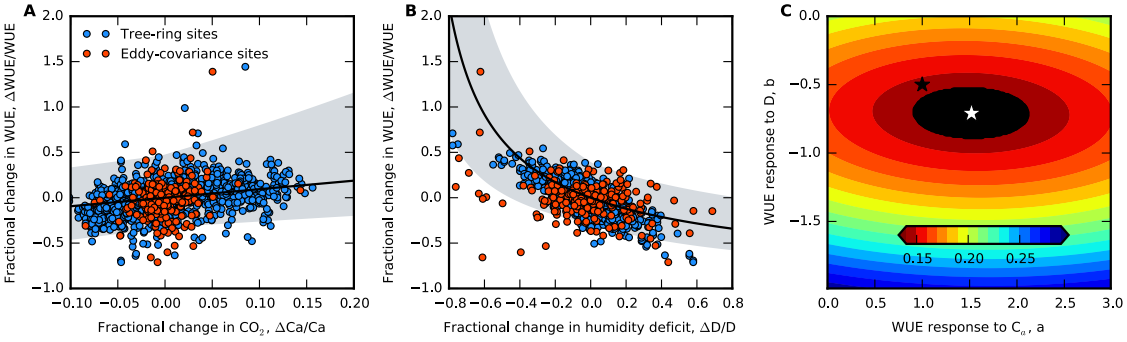

Figure 1. Water Use Efficiency (WUE) from tree-ring and eddy-covariance observations. The relationship between the observed fractional change in WUE and the fractional change in (A) CO_2 concentration and (B) humidity deficit of both datasets is fitted to Equation 3,with best-fit values for *a* (1.51±0.57) and *b* (-0.72±0.16). (C) The colors show the root mean square error (RMSE) of the simulated vs. observed fractional change in WUE as a function of *a* and *b*, with the black area representing the best parameters within 5% of the RMSE of the best fit (white star). The black star represents the values according to the optimality hypothesis.

Earth Syst. Dynam. Discuss., doi:10.5194/esd-2016-4, 2016
Manuscript under review for journal Earth Syst. Dynam.
Published: 22 February 2016

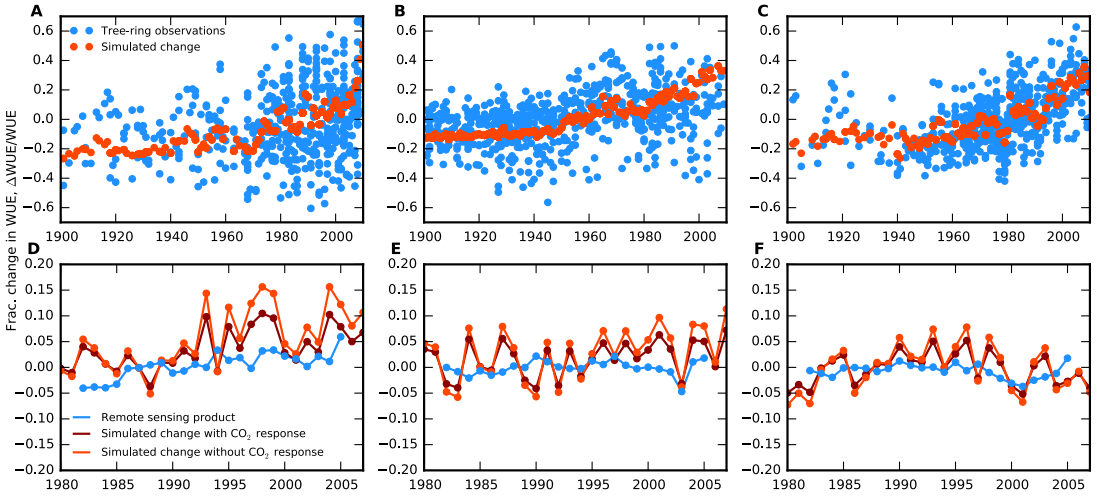

Figure 2. Comparison of estimated Water Use Efficiency trends to independent observations. Simulated fractional change in *WUE* (orange) compared to observations for three tropical tree-ring sites in Bolivia (A), Cameroon (B) and Thailand (C) (blue, van der Sleen 2015). Simulated fractional change in *WUE* for (D) Western North America, (E) Western Europe and (F) East Asia, with (dark red) and without (orange) CO_2 effect, compared to the *WUE* trend derived from a remote sensing product of carbon uptake and water loss (Lin 2015). The location of the tree-ring sites is presented in Fig. S1 and the regions D-F are as in Fig. 5.

Earth Syst. Dynam. Discuss., doi:10.5194/esd-2016-4, 2016
Manuscript under review for journal Earth Syst. Dynam.
Published: 22 February 2016

Earth System Dynamics
Discussions
Open Access
EGU

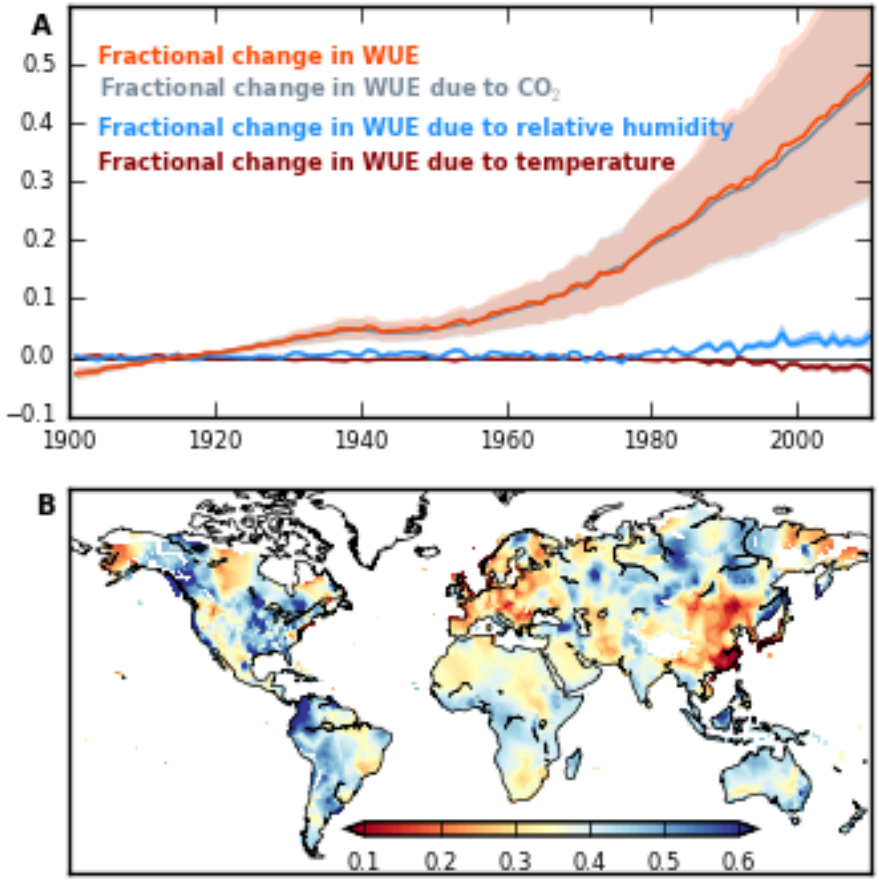

412

413 **Figure 3.** 20th century fractional change of Water Use Efficiency (*WUE*). (A) Time series of the
414 estimated global fractional change in *WUE* (orange, relative to the average over 1901-1930)
415 partitioned into the effects of changes in CO_2, relative humidity and temperature. (B) Spatial pattern
416 of the estimated fractional change in *WUE* between 1901-1930 and 2001-2010. These calculations
417 use observed monthly surface air temperature and vapour pressure (Harris et al. 2013) during the
418 growing season, and annual atmospheric CO_2 concentrations at Mauna Loa (Keeling et al. 1976).

419

420

Earth Syst. Dynam. Discuss., doi:10.5194/esd-2016-4, 2016
Manuscript under review for journal Earth Syst. Dynam.
Published: 22 February 2016

Earth System Dynamics
Discussions
Open Access
EGU

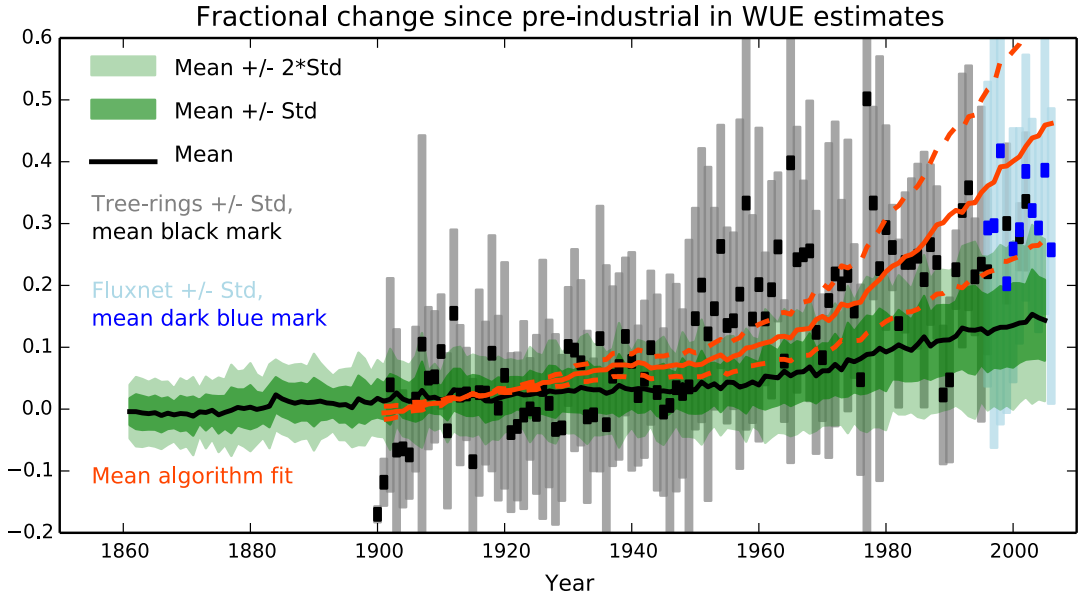

421

422 **Figure 4.** Comparison of measured and modeled fractional changes in WUE from 1860 to 2010.
423 Estimates from tree-rings and eddy-covariance data are shown by the black and blue points
424 respectively, with the bars in each case showing +/-1 standard deviation about the mean response.
425 The results from complex coupled Earth System Models are shown by the black continuous line and
426 the green plume (with dark green showing one standard deviation and light green showing two
427 standard deviations). The algorithm presented in this paper, which estimates fractional WUE
428 changes from changes in CO_2 concentration and humidity deficit alone (equation 6), is shown by
429 the orange lines. To enable the comparison between these different estimates, we normalized over
430 common overlapping periods (for the tree-ring data and model simulations – 1900-1930; for the
431 tree-ring and eddy-covariance data – the period of overlap when at least 3 eddy-covariance sites are
432 available).

433

434

Earth Syst. Dynam. Discuss., doi:10.5194/esd-2016-4, 2016
Manuscript under review for journal Earth Syst. Dynam.
Published: 22 February 2016

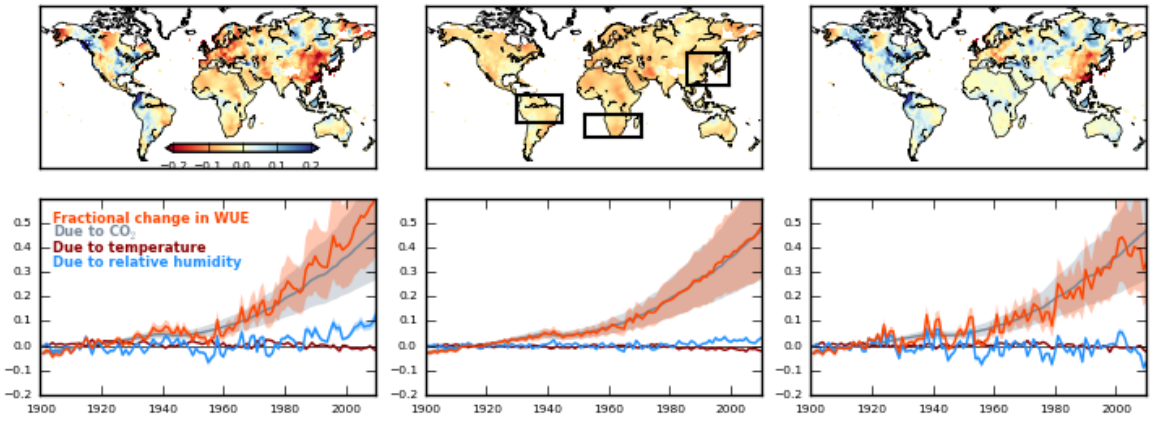

435

436 **Figure 5.** Changes in *WUE* arising from climate variables. Spatial patterns of the fractional changes
437 in WUE arising from changes in (A) climate, i.e. both temperature and relative humidity (*RH*)
438 together, (B) temperature alone, and (C) *RH* alone, between 1901-1930 and 2001-2010. Time-series
439 are as in Fig. 2 for (D) Western North America, (E) Western Europe and (F) East Asia, which show
440 the large regional and temporal variations in these climate-driven changes in *WUE*.